



THE UNIVERSITY *of* EDINBURGH

Edinburgh Research Explorer

CCL2 recruits inflammatory monocytes to facilitate breast-tumour metastasis

Citation for published version:

Qian, B, Li, J, Zhang, H, Kitamura, T, Zhang, J, Campion, LR, Kaiser, EA, Snyder, LA & Pollard, JW 2011, 'CCL2 recruits inflammatory monocytes to facilitate breast-tumour metastasis' Nature, vol 475, no. 7355, pp. 222-225., 10.1038/nature10138

Digital Object Identifier (DOI):

[10.1038/nature10138](https://doi.org/10.1038/nature10138)

Link:

[Link to publication record in Edinburgh Research Explorer](#)

Document Version:

Author final version (often known as postprint)

Published In:

Nature

Publisher Rights Statement:

Published in final edited form as:
Nature. 2011 June 8; 475(7355): 222–225.
doi: 10.1038/nature10138

General rights

Copyright for the publications made accessible via the Edinburgh Research Explorer is retained by the author(s) and / or other copyright owners and it is a condition of accessing these publications that users recognise and abide by the legal requirements associated with these rights.

Take down policy

The University of Edinburgh has made every reasonable effort to ensure that Edinburgh Research Explorer content complies with UK legislation. If you believe that the public display of this file breaches copyright please contact openaccess@ed.ac.uk providing details, and we will remove access to the work immediately and investigate your claim.





Published in final edited form as:

Nature. ; 475(7355): 222–225. doi:10.1038/nature10138.

CCL2 recruits inflammatory monocytes to facilitate breast tumor metastasis

Bin-Zhi Qian¹, Jiufeng Li¹, Hui Zhang¹, Takanori Kitamura¹, Jinghang Zhang², Liam R. Campion³, Elizabeth A. Kaiser³, Linda A. Snyder³, and Jeffrey W. Pollard^{1,*}

¹Department of Developmental and Molecular Biology, Center for the Study of Reproductive Biology and Woman's Health, Albert Einstein College of Medicine, NY, NY 10461, USA

²Flow Cytometry Core Facility, Albert Einstein College of Medicine, NY, NY 10461, USA

³Ortho Biotech Oncology R&D, 145 King of Prussia Road, Radnor, PA 19087, USA

Abstract

Macrophages abundantly found in the tumor microenvironment enhance malignancy¹. At metastatic sites a distinct population of metastasis associated macrophages (MAMs) promote tumor cell extravasation, seeding and persistent growth². Our study has defined the origin of these macrophages by showing Gr1⁺ inflammatory monocytes (IMs) are preferentially recruited to pulmonary metastases but not primary mammary tumors, a process also found for human IMs in pulmonary metastases of human breast cancer cells. The recruitment of these CCR2 (receptor for chemokine CCL2) expressing IMs and subsequently MAMs and their interaction with metastasizing tumor cells is dependent on tumor and stromal synthesized CCL2 (FigS1). Inhibition of CCL2/CCR2 signaling using anti-CCL2 antibodies blocks IM recruitment and inhibits metastasis in vivo and prolongs the survival of tumor-bearing mice. Depletion of tumor cell-derived CCL2 also inhibits metastatic seeding. IMs promote tumor cell extravasation in a process that requires monocyte-derived VEGF. CCL2 expression and macrophage infiltration are correlated with poor prognosis and metastatic disease in human breast cancer (Fig S2)³⁻⁶. Our data provides the mechanistic link between these two clinical associations and indicates new therapeutic targets for treating metastatic breast disease.

To understand the origin of macrophages in primary tumors and their metastatic sites we measured monocyte trafficking. Mouse monocytes were identified by their expression of CD11b and CD115 (Fig. S3a) and sorted by FACS into sub-populations of Gr1⁺/Ly6C⁺ IMs and Gr1⁻/Ly6C⁻ resident monocytes (RMs)^{7,8} (Fig. S3b-d). 10⁵ of each monocyte population which have similar *Csf1r*-GFP expression as a reporter (Fig. S3b) were adoptively transferred⁹⁻¹¹ into syngeneic FVB mice bearing autochthonous late stage PyMT mammary tumors with spontaneous pulmonary metastases (Fig. 1a). 18 hours after adoptive transfer the ratio of recovered GFP⁺ (Fig. S3e) IMs over RMs from the same donor were determined to measure their relative recruitment. This indicated similar numbers of donor cells in the blood (showing equivalent availability), but in the primary tumor RMs are preferentially recruited while in pulmonary metastases, IMs are preferentially recruited with greater than 3-fold enrichment (Fig. 1b). Consistent with this, a significant population of endogenous IMs is identified in metastasis-bearing but not normal lung (Fig. S4a). This preferential IM recruitment in lung is not observed in 7-week-old PyMT mice bearing pre-metastatic mammary tumors (Fig. S4b). In experimentally induced pulmonary foci of i.v.

*Corresponding author: Jeffrey W Pollard, Department of Developmental and Molecular Biology, Albert Einstein College of Medicine, Bronx, NY 10461, USA. Tel: 718-430-2090, Fax: 718-430-8972, pollard@acem.yu.edu .

injected Met-1 cells¹², IMs are also preferentially recruited (Fig. S4c). GFP labeled cells are readily detectable in pulmonary metastases 5 days after transfer (data not shown) and within two days a significant portion of them have differentiated into F4/80+CD11b+Gr1-MAMs² that are not seen in normal lungs (Fig. S4d). To test if IMs were recruited early in the metastasis process, we transferred monocyte populations 7 hours after i.v. injection of Met-1 cells, a time point chosen before significant tumor-macrophage interaction and tumor cell extravasation². Compared with control lungs, the recruitment of IMs to the tumor cell-challenged lung dramatically increased with the ratio of IMs over RMs increasing over 5-fold (Fig. 1c). However, this preferential recruitment of IMs was not observed following i.v. injection with PBS or latex beads as a control for injection or particle lodgment (data not shown and Fig. S4e). Consistent with this early recruitment of IMs, CCR2^{hi} MAMs were preferentially recruited to lungs 36 hours after tumor cell inoculation². However at this time B cells and T cells, including Foxp3+ Treg cells were not differentially recruited (Fig. S5a-c and data not shown). These data indicate that MAMs are derived from IMs that are specifically recruited early during pulmonary metastases before other immune cells.

Distinct chemokine signals recruit monocytes⁷ with IMs responding to CCL2^{10,11}. Lung metastases of PyMT tumor homogeneously express CCL2, in contrast to heterogeneous expression in primary tumors (Fig. S6a-d). IMs but not RMs have high level of CCR2 expression (Fig. S6e). Neutralizing CCL2 using anti-mouse CCL2 Ab¹³ significantly inhibited the recruitment of IMs to lungs challenged with metastatic tumor cells (Fig. 1d) and the increase in MAMs to the metastatic site (Fig. S4f). Other CCR2 expressing leukocytes (sub-population of T cell) and Treg cells in this model are unaffected by anti-CCL2 Ab treatment (Fig. S5d). Furthermore, preferential recruitment of IMs to tumor cell challenged lung was completely abrogated with adoptive transfer of monocytes sorted from CCR2 null mutant (KO) mice (Fig. S6f).

The pattern of human monocytes recruitment *in vivo* to tumors is unknown. To test this, human CD14+CD16- IMs and CD14^{lo}CD16+ RMs⁹ were sorted from enriched CD14+ cells from peripheral blood of healthy donors (Fig. S7a). 10⁵ cells of each population were adoptively transferred into pairs of nude mice supplemented with recombinant human CSF-1 that is essential for monocyte/macrophage survival (Fig. S7e). Human monocytes were quantified using FACS analysis with anti-human CD45 antibody 18 hours after adoptive transfer (Fig. S7b). In normal mice transferred with monocytes from the same donor there are comparable numbers of human IMs and RMs in the circulation and recruited to the lung but about twice the numbers of IMs compared to RMs in the spleen (Fig. 1e, open bars). In mice given an i.v. injection of human MDA-MB-231-derived metastatic 4173 breast cancer cells¹⁴ 7 hours before monocyte transfer, the ratio of the two monocyte populations in blood and spleen was similar to normal mice, but in the lungs IMs increased in ratio of >6-fold (Fig. 1e). In established pulmonary metastases derived from orthotopically injected 4173 cells, IMs were also preferentially recruited with a 5-fold increased ratio compared to normal lungs (Fig. S7d). Mouse IMs were also preferentially recruited to 4173 cells challenged lungs (data not shown). Human IMs express CCR2 with RMs expressing minimal levels of the receptor (Fig. S7c). Neutralizing host CCL2 using anti-mouse CCL2 Ab significantly reduced the recruitment of human IMs into lungs challenged with 4173 cells without change in the circulation or spleen (Fig. 1f). Treatment with an antibody specific to human CCL2¹⁵ also inhibited IM recruitment (Fig. S7f) indicating the importance of CCL2 from both tumor and the target organ. This indicates that human IMs respond to the same CCL2/CCR2 signaling as the mouse cells for their specific recruitment during pulmonary metastasis

To test the effect of blocking IM recruitment on metastatic potential, we performed experimental metastasis assays with Met-1 cells mice treated with anti-mouse CCL2 or

control Ab shortly before the tumor cell injection. This treatment reduced the total metastasis burden due to a significantly reduced number of metastasis nodules (Fig. 2a, b). Specific antibody to mouse CCL12, another ligand of mouse CCR2, had no effect on Met-1 cell metastasis (Fig. S8). This indicates that the specific CCL2-mediated IM recruitment is critical for tumor cell pulmonary seeding.

Extravasation is a critical step for tumor cell metastatic seeding in lung². We used an intact lung imaging system¹⁶ to test the role of CCL2 recruited IMs in tumor cell extravasation. *Csf1r*-EGFP transgenic mice were injected i.v. with CFP-expressing Met-1 cells and harvested after 24 hours. Quantification of 3D reconstructed confocal images (Fig. 2c, d, Movie S1 and S2) shows that the number of macrophages directly interacting with tumor cells was significantly reduced by CCL2 neutralizing Ab compared with control Ab (Fig. 2e). Importantly, tumor cell extravasation was delayed and less efficient following IM blockade (Fig. 2f). Tumor cell extravasation involves cross talk between tumor cells, endothelial cells, basement membrane and macrophages. In an in vitro trans-endothelia migration assay (Fig. S9a)¹⁷ tumor cell trans-endothelial migration is enhanced ~5-fold by mouse bone marrow derived macrophages (BMMs) located on the basal-lateral side of the endothelial monolayer. This effect is blocked by anti-mouse CCL2 neutralizing antibody but not control antibody (Fig. S9b). All three cell-types express CCL2, while only the macrophages express CCR2 (Fig. S9c) indicating that only macrophages respond to the CCL2 chemokine signaling. In confirmation of this macrophages from CCR2 KO mice are not capable of promoting tumor cell trans-endothelia migration (Fig. S9d). Importantly, FACS sorted IMs but not RMs significantly promoted tumor cell trans-endothelia migration that was also inhibited by anti-mouse CCL2 neutralizing antibody (Fig. 2g, h).

Total CCL2 blockade (both mouse and human) inhibited spontaneous lung metastasis of orthotopically injected MDA-MB-231 cells (Fig. 3a). Both tumor cell and host secreted ligands contribute to metastatic efficiency, since both anti-human and -mouse Ab alone significantly inhibit 4173 experimental metastasis (Fig. 3b) without affecting tumor cell proliferation in vitro (data not shown). This conclusion was also confirmed by knocking down CCL2 using siRNAs in 4173 cells which significantly reduced lung colonization in experimental metastasis assays (Fig. S10e, f). Consistent with this, a similar CCL2 knockdown in Met-1 cells did not affect tumor cell proliferation in vitro, but significantly inhibited their metastatic efficiency (Fig. S10a-c). In vitro 4173 trans-endothelia migration is also promoted by human IMs and inhibited by neutralizing either human or mouse CCL2 with specific Abs (Fig. 3c-e). These data indicate that tumor cell and target organ secreted CCL2 work together to promote tumor cell extravasation and metastatic seeding via action on IM recruitment. Consistent with the role of microenvironmental synthesized CCL2 in the lung, bone metastasis of MDA-MB-231 cells also recruit IMs and inhibition of CCL2 inhibits metastatic progression. In contrast liver metastasis of Met-1 cells did not recruit IMs and CCL2 inhibition did not reduce metastasis (data not shown). Furthermore, CCL2 blockade 2 days after i.v. injection of MDA-MB-231 cells reduces lung tumor burden and prolongs survival of mice indicating the importance of continuous recruitment of IM and their differentiation into MAMs for persistent metastatic growth (Fig. 3f, g).

To determine mechanism of the effects of IMs on tumor cell extravasation we analyzed the transcriptomes of RMs and IMs¹⁸. Among the differentially regulated genes VEGF is highly expressed by IMs, a fact we verified (Fig. S11a). To conditionally ablate VEGF in myeloid cells to test its role in the metastatic process, we generated a transgenic mouse expressing tamoxifen inducible Mer-iCre fusion protein driven by the *Csf1r* promoter crossed with *VEGF^{flox/flox}* mice¹⁹. Inducible ablation of *Vegf* was achieved in cultured BMMs treated with 4-hydroxytamoxifen (Fig. 4a) and these *Vegf* KO BMMs compared to control BMM are unable to promote tumor cell trans-endothelial migration and do not enhance

permeability of the endothelial monolayer (Fig. 4b, c), a process important for metastasis²⁰. In vivo injection of tamoxifen specifically ablates *Vegf* in monocytes without ablation in other circulating immune cells (Fig. 4d). This monocyte-specific depletion of VEGF significantly inhibited Met-1 cell experimental metastasis potential and seeding efficiency (Fig. 4e and S11b). Adoptive transfer experiments indicated that *Vegf* KO IMs infiltrate Met-1 lung metastasis at a comparable level as *Vegf*^{fllox} IMs, showing that this molecule is not required for IM recruitment (Fig. S11c). Importantly, co-injection of Met-1 cells and WT IMs into inducible macrophage VEGF knockout mice restored the tumor cell metastatic potential (Fig. 4f).

Thus, these experiments have indicated that CCL2 synthesized by metastatic tumor cells and the target site tissue stroma is critical for recruitment of a sub-population of CCR2 expressing monocytes that enhance the subsequent extravasation of the tumor cells. Mechanistically this is at least in part through targeted delivery of molecules such as VEGF that promote extravasation. IMs are continually recruited by a CCL2 mechanism and differentiate into macrophages that promote the subsequent growth of metastatic cells. These data together with the clinical associations of CCL2 over-expression in human cancer noted above strongly argue for therapeutic approaches targeted against monocyte recruitment and function.

Methods Summary

Monocytes trafficking into primary tumors and their metastases were studied by adoptive transfer of mouse (Ly6C/Gr1⁺ or Ly6C/Gr1⁻) or human (CD14⁺CD16⁺ and CD16⁻) monocytes using MMTV-PyMT autochthonous, human and mouse experimental metastasis and human orthotopic tumor models. Monocytes and macrophages were recovered by enzymatic disaggregation of the tumors followed by FACS analysis. To test mechanisms behind monocyte recruitment and the effect of inhibition of this trafficking on metastasis anti-mouse or human neutralizing CCL2 antibodies or *Ccr2* null mutant mice were used. In order to ablate VEGF expression in monocytes a myeloid specific (*Csf1r* promoter) tamoxifen inducible Cre expressing strain was crossed with *VEGF*^{fllox/fllox} mice and gene ablation induced by tamoxifen. Effects of monocyte depletion on tumor cell extravasation using Met-1, a FVB PyMT tumor derived metastatic cell line, was determined using an ex vivo intact lung imaging system and an in vitro extravasation assay.

Supplementary Material

Refer to Web version on PubMed Central for supplementary material.

Acknowledgments

Conceived and designed the experiments: BZQ, LAS, JWP. Performed the experiments: BZQ, JL, HZ, TK, JZ, LRC, EAK. Analyzed the data: BZQ, JL, LAS, JWP. Wrote the paper: BZQ, LAS, JWP. This work was supported by grants from the NIH to JWP (NIH PO1 CA100324 and RO1 CA131270) and to the Albert Einstein Cancer Center Core (P30 CA 13330). We thank Dr. Joan Massague, MSKCC, for 4173 and 1833 cells and Dr. Napoleone Ferrara, Genetech, for the *Vegf*^{fllox/fllox} mice. We also thank Paul Marsters for certain statistical analyses, Mark Thompson, Frank Shi, Catherine Ferrante, Francis McCabe, Hillary Millar-Quinn and Diana Wiley for helpful discussions and technical assistance.

Appendix

Methods

Animals

All procedures involving mice were conducted in accordance with National Institutes of Health regulations concerning the use and care of experimental animals. The study of mice was approved by the Albert Einstein College of Medicine and Ortho Biotech R&D Institute Animal Care and Use Committees. Transgenic mice expressing the Polyoma Middle T (PyMT) oncogene under the control of MMTV LTR were provided by Dr. W.J. Muller (McMaster University, Ontario, Canada) and bred in house. FVB (*Tg(Csf1r-EGFP)1Jwp*) mice have been previously reported to have the whole mononuclear phagocyte system labeled²¹. BL6 *Ccr2^{tm1Jfc}/J* mice were purchased from The Jackson Laboratory. FVB macrophage specific (*Csf1r* promoter) tamoxifen inducible Cre expressing *Tg(Csf1r-Mer-iCre-Mer)1Jwp* transgenic mouse strain was generated and crossed with *VEGF^{fllox/fllox}* mice (kind gift from Dr. Napoleone Ferrara, Genentech). VEGF knock-out in myeloid cells was induced by s.c. injection of 3 ug tamoxifen per mouse daily for 2 days before sorting for blood leukocytes or tumor cell injection.

Metastasis assay

8-week-old FVB females and 6-week-old female nude mice were used for lung experimental metastasis assays with i.v. injection of 5×10^5 Met-1 cells and 10^6 MDA-MB-231-derived LM2 human breast cancer cells, 4173²², respectively. If not specified, all animals were killed 2 weeks after i.v. injection of Met-1 cells or 4 weeks of human tumor cells for optimal metastatic burden. In experimental metastasis assays, antibodies were given at 10 mg/kg body weight via i.p. injection 3 hours before tumor cell injection for one time treatments, or twice a week afterwards in prolonged treatment, if not specified. For paraffin sections, lungs were injected with 1.2 ml of 10% neutral buffered formalin by tracheal cannulation in order to fix the inner airspaces and inflate the lung lobes. Lungs were excised and fixed in formalin overnight. A precise stereological method²³ with modification was used for lung metastasis quantification. Briefly, paraffin-embedded lungs were systematically sectioned through the entire lung with one 5 um section taken in every 0.5 mm lung thickness. All sections were stained with H&E and images were taken using a Zeiss SV11 microscope with a Retiga 1300 digital camera and analyzed using ImageJ²⁴. Mets index equals total Mets volume normalized to total lung volume and Mets number index equals number of Mets nodules per mm² of lung area. Realtime PCR quantification of human tumor cell burden were performed as reported using human specific primers²⁵. For spontaneous lung metastasis, 2.5×10^6 MDA-MB-231 or 10^6 LM2 tumor cells were orthotopically injected into the inguinal mammary gland of SCID beige or nude mice respectively. Anti-mouse CCL2 and CCL12²⁶ and anti-human CCL2²⁷ antibodies specifically neutralize only their respective target molecules and were provided by Centocor Inc., PA, together with the control antibody. In spontaneous metastasis assays, antibody treatment began on day 3 after tumor cell intra-mammary gland injection with 20 mg/kg body weight of each antibody and continued twice a week thereafter. When each group reached a mean primary tumor volume of $\sim 1000 \text{ mm}^3$, the mice were euthanized. Lungs were perfused with India ink and placed in Fekete's solution. Lung metastases were counted in a blinded fashion. All in vivo experiments were at least two independent experiments with 3-10 mice for each group.

Adoptive transfer

CD115⁺F4/80⁺CD11b⁺Ly6C/Gr1⁺ and Ly6C/Gr1⁻ BM monocytes were sorted from FVB *Csf-1r-EGFP* and adoptively transferred into FVB mice. 10^5 of either cells were transferred into mice bearing mammary tumors and/or pulmonary metastases. Monocytes were sorted

using the same protocol from CCR2 null mutant mice (KO) mice and labeled with CellTracker™ (Invitrogen) following manufacturer's instruction, before adoptive transfer into nude mice. Fresh human CD14⁺ peripheral monocytes were purchased from All Cells LLC. CA. 10⁵ CD14⁺CD16⁻ and CD14⁺CD16⁺ cells were FACS sorted and i.v. transferred into nude mice supplemented with 2×10⁶ units recombinant human CSF-1 via s.c. injection. In indicated experiments, specified antibodies were given at 10 mg/kg body weight 3 hours before monocyte adoptive transfer.

FACS analysis and antibodies

For FACS analysis, lungs or whole mice were perfused thoroughly with cold PBS before harvest, then lungs were minced on ice and digested with enzyme mix of Liberase and Dispase (Invitrogen, CA). Blood was drawn by cardiac puncture. Red blood cells were removed using RBC Lysis buffer (eBioscience, CA). Cells were blocked using anti-mouse CD16/CD32 antibody (eBioscience, CA) for mouse cells or 10% goat serum for human cells before antibody staining. Antibodies used were: anti-mouse CD45 (30-F11), CD11b (M1/70), Gr1 (RB6-8C5), CD115 (AFS98), Foxp3 (FJK-16s; eBioscience), CD3 (145-2C11), Ly6C (HK1.4; Biolegend), CD25 (PC61), CD62L (MEL-14), IL4Ra (mIL4R-M1), CD4 (GK1.5), CD8a (53-6.7), Ly6G (1A8; BD Pharmingen) and F4/80 (Cl:A3-1; AbD Serotec); anti-human CD14 (Tük4), CD16 (3G8; Invitrogen) and CD45 (HI30; BioLegend), CCR2 (48607; R&D Systems). FACS analysis was performed on a LSRII cytometer (BD Biosciences) and data were analyzed using Flowjo software (TreeStar, OR). Single cells gating using FSC/W and SSC/W and dead cells exclusion with DAPI staining were performed routinely during analysis. Mouse CCL2 was stained using specific Ab (R-17; Santa Cruz) following a standard immunohistochemistry protocol.

Cell culture and *in vitro* extravasation assay

All cells were cultured in Dulbecco's modified Eagle's medium (DMEM) supplemented with 10% fetal bovine serum. The extravasation assay was performed as previously described^{28,29} with modifications. Briefly, 2×10⁴ endothelial cells, 3B-11 (ATCC), were plated into the upper chamber of GFR Matrigel™ invasion chamber (BD Biosciences) in DMEM with 10% (v/v) FBS. A monolayer was formed in 2 days and verified by microscopy. 10⁴ bone marrow derived macrophages (BMMs) or FACS sorted monocytes were loaded to the basolateral side of the insert and put into plate well with DMEM with 10% FBS and 10⁴ unit/ml Colony stimulating factor-1 (CSF-1) to allow attachment. VEGF knockout BMMs derived from *Csf-1r-Mer-iCre-Mer:VEGF^{lox/lox}* mouse were induced by treating the cells with 1 μM 4-hydroxyl-tamoxifen for 7 days after BM isolation. 2×10⁴ CellTracker™ CMRA (Invitrogen) stained Met-1 cells were loaded into the insert with DMEM in 0.5% (v/v) FBS and 10⁴ unit/ml CSF-1. CCL2 neutralizing antibody and control antibody were used at 5 μg/ml applied to both sides of the insert. Plates were incubated under normal tissue culture conditions for 36-48 hours before being fixed with 1% (w/v) paraformaldehyde. Tumor cell trans-endothelial migration was quantified by counting the number of cells that migrated through the insert under a fluorescent microscope (6-10 different randomly selected fields in each insert) and expressed as cell number per 20X field if not specified. Permeability assay was performed by loading 4% (w/v) Evan's blue labeled BSA to the upper chamber with pre-formed endothelial monolayer of 3B-11 cells and measuring absorption of the phenol-red free medium of the lower chamber at 650 nm after 30 minutes incubation in normal culturing conditions. All *in vitro* experiments were at least three independent experiments with duplicates or triplicates measures.

Molecular Biology

A 97-mer oligo containing the shRNA targeting CCL2 mRNA sequence from nucleotides 166 was cloned into the miR30 context in retroviral vector P2GM³⁰ to knockdown CCL2 in

Met-1 cells. A 97-mer oligo containing the shRNA targeting human CCL2 mRNA sequence from nucleotides 255 is cloned into the miR30 context in retroviral vector P2GM to knockdown CCL2 in 4173 cells. For RT-PCR of mouse CCL2 expression, primers CCCAATGAGTAGGCTGGAGA and AAAATGGATCCACACCTTGC were used, and for CCR2, CCTGCAAAGACCAGAAGAGG and GTGAGCAGGAAGAGCAGGTC. All realtime-PCR was performed on an MJ Research DNA Engin2 Opticon realtime PCR machine using SYBR master mix (Invitrogen). Primers used were: mouse CCL2 primers GTTGGCTCAGCCAGATGCA and AGCCTACTCATTGGGATCATCTTG; mouse CCR2 TTTGTTTTTGCAGATGATTCAA and TGCCATCATAAAGGAGCCAT; mouse uPA ACAGATAAGCGGTCTCCAG and GCCCACTACTATGGCTCTG; mouse VEGF AATGCTTTCTCCGCTCTGAA and GCTTCCTACAGCACAGCAGA; mouse VEGF exon 3 ACATCTTCAAGCCGTCCTGT and CTGCATGGTGATGTTGCTCT; human CCL2: AGGTGACTGGGGCATTGAT and GCCTCCAGCATGAAAGTCTC. To verify mouse VEGF exon 3 knockout, primers that flank this exon: GCTGCACCCACGACAGAAGG and TGAGGTTTGATCCGCATGAT were used.

Ex vivo whole lung imaging

A well-established intact lung microscopy technique^{31,32} was applied to observe tumor cells, macrophages, and blood vessels in the mouse lungs. CFP-expressing Met-1 cells prepared by retro-virus infection of a CMV promoter-CFP vector were injected i.v. into the tail vein of each mouse. At the time indicated, mice were anesthetized and injected with 10 ug Alexa Fluor® 647 conjugated anti-mouse CD31 antibody (BioLegend, CA). Five minutes later, the mouse was put under artificial ventilation through trachea cannulation. The lung was cleared of blood by gravity perfusion through the pulmonary artery with artificial medium [Kreb-Ringer bicarbonate buffer with 5% dextran and 10mmol/L glucose (pH 7.4)]. The heart–lung preparation was dissected en bloc and placed in a specially designed plexiglass chamber with a port to the artificial cannula. The lung rested on a plexiglass window at the bottom of the chamber with the posterior surface of the lung touching the plexiglass. The lung was ventilated throughout the experiment with 5% CO₂ in medical air and perfused by gravity perfusion except during imaging. Three to five animals were imaged for each time point and 10 to 20 unrelated fields were imaged for each animal.

Images were collected with a Leica TCS SP2 AOBS confocal microscope (Mannheim, Germany) with 60X oil immersion optics. Laser lines at 458 nm, 488 nm and 633 nm for excitation of CFP, GFP and AF647 were provided by an Ar laser and a HeNe laser. Detection ranges were set to eliminate crosstalk between fluorophores. Three-dimensional reconstruction was performed using Volocity™ (Improvision Inc., MA).

Statistical analysis

Statistical analysis methods employed were standard two-tailed Student's t test for two data sets and ANOVA followed by Bonferroni/Dunn post-hoc tests for multiple data sets using Prism (GraphPad Inc.), except for human monocyte transfer with antibody treatment where paired t test was used because of variations among different donors. For spontaneous metastasis assay of MDA-MB-231 cells, percent differences in numbers of lung metastases were compared between groups using parametric survival regression methods, with metastasis counts greater than 100 considered censored at 100. P values below 0.05 (*), <0.01 (**) and < 0.001 (***) were deemed as significant and highly significant, respectively.

References

21. Qian B, et al. A distinct macrophage population mediates metastatic breast cancer cell extravasation, establishment and growth. *PLoS ONE*. 2009; 4:e6562. doi:10.1371/journal.pone.0006562. [PubMed: 19668347]
22. Minn AJ, et al. Genes that mediate breast cancer metastasis to lung. *Nature*. 2005; 436:518–524. [PubMed: 16049480]
23. Nielsen BS, et al. A precise and efficient stereological method for determining murine lung metastasis volumes. *The American journal of pathology*. 2001; 158:1997–2003. [PubMed: 11395377]
24. Abramoff MD, Magelhaes PJ, Ram SJ. Image Processing with Image. *J. Biophotonics International*. 2004; 11:36–42.
25. Havens AM, et al. An in vivo mouse model for human prostate cancer metastasis. *Neoplasia (New York, N.Y.)*. 2008; 10:371–380.
26. Tsui P, et al. Generation, characterization and biological activity of CCL2 (MCP-1/JE) and CCL12 (MCP-5) specific antibodies. *Hum Antibodies*. 2007; 16:117–125. [PubMed: 18334747]
27. Carton JM, et al. Codon engineering for improved antibody expression in mammalian cells. *Protein Expr Purif*. 2007; 55:279–286. doi:S1046-5928(07)00147-7 [pii]10.1016/j.pep.2007.05.017. [PubMed: 17646110]
28. Brandt B, et al. 3D-extravasation model - selection of highly motile and metastatic cancer cells. *Seminars in cancer biology*. 2005; 15:387–395. [PubMed: 16054390]
29. Ma C, Wang X-F. In Vitro Assays for the Extracellular Matrix Protein-Regulated Extravasation Process. *Cold Spring Harbor Protocols*. 2008; 2008.pdb.prot5034-, doi:10.1101/pdb.prot5034.
30. Stern P, et al. A system for Cre-regulated RNA interference in vivo. *Proceedings of the National Academy of Sciences of the United States of America*. 2008; 105:13895–13900. [PubMed: 18779577]
31. Al-Mehdi AB, et al. Intravascular origin of metastasis from the proliferation of endothelium-attached tumor cells: a new model for metastasis. *Nat Med*. 2000; 6:100–102. [PubMed: 10613833]
32. Im JH, et al. Coagulation facilitates tumor cell spreading in the pulmonary vasculature during early metastatic colony formation. *Cancer research*. 2004; 64:8613–8619. [PubMed: 15574768]

References

1. Qian BZ, Pollard JW. Macrophage diversity enhances tumor progression and metastasis. *Cell*. 2010; 141:39–51. doi:S0092-8674(10)00287-4 [pii]10.1016/j.cell.2010.03.014. [PubMed: 20371344]
2. Qian B, et al. A distinct macrophage population mediates metastatic breast cancer cell extravasation, establishment and growth. *PLoS ONE*. 2009; 4:e6562. doi:10.1371/journal.pone.0006562. [PubMed: 19668347]
3. Ueno T, et al. Significance of macrophage chemoattractant protein-1 in macrophage recruitment, angiogenesis, and survival in human breast cancer. *Clin Cancer Res*. 2000; 6:3282–3289. [PubMed: 10955814]
4. Valkovic T, Lucin K, Krstulja M, Dobi-Babic R, Jonjic N. Expression of monocyte chemotactic protein-1 in human invasive ductal breast cancer. *Pathol Res Pract*. 1998; 194:335–340. [PubMed: 9651946]
5. Saji H, et al. Significant correlation of monocyte chemoattractant protein-1 expression with neovascularization and progression of breast carcinoma. *Cancer*. 2001; 92:1085–1091. [PubMed: 11571719]
6. Rhodes DR, et al. ONCOMINE: a cancer microarray database and integrated data-mining platform. *Neoplasia (New York, N.Y.)*. 2004; 6:1–6.
7. Geissmann F, et al. Blood monocytes: distinct subsets, how they relate to dendritic cells, and their possible roles in the regulation of T-cell responses. *Immunology and cell biology*. 2008; 86:398–408. doi:icb200819 [pii]10.1038/icb.2008.19. [PubMed: 18392044]

8. Geissmann F, et al. Development of monocytes, macrophages, and dendritic cells. *Science (New York, N.Y.)*. 2010; 327:656–661. doi:327/5966/656 [pii]10.1126/science.1178331.
9. Geissmann F, Jung S, Littman DR. Blood monocytes consist of two principal subsets with distinct migratory properties. *Immunity*. 2003; 19:71–82. [PubMed: 12871640]
10. Getts DR, et al. Ly6c+ “inflammatory monocytes” are microglial precursors recruited in a pathogenic manner in West Nile virus encephalitis. *The Journal of experimental medicine*. 2008; 205:2319–2337. doi:jem.20080421 [pii]10.1084/jem.20080421. [PubMed: 18779347]
11. Palframan RT, et al. Inflammatory chemokine transport and presentation in HEV: a remote control mechanism for monocyte recruitment to lymph nodes in inflamed tissues. *The Journal of experimental medicine*. 2001; 194:1361–1373. [PubMed: 11696600]
12. Borowsky AD, et al. Syngeneic mouse mammary carcinoma cell lines: two closely related cell lines with divergent metastatic behavior. *Clinical & experimental metastasis*. 2005; 22:47–59. [PubMed: 16132578]
13. Tsui P, et al. Generation, characterization and biological activity of CCL2 (MCP-1/JE) and CCL12 (MCP-5) specific antibodies. *Hum Antibodies*. 2007; 16:117–125. [PubMed: 18334747]
14. Minn AJ, et al. Genes that mediate breast cancer metastasis to lung. *Nature*. 2005; 436:518–524. [PubMed: 16049480]
15. Carton JM, et al. Codon engineering for improved antibody expression in mammalian cells. *Protein Expr Purif*. 2007; 55:279–286. doi:S1046-5928(07)00147-7 [pii]10.1016/j.pep.2007.05.017. [PubMed: 17646110]
16. Al-Mehdi AB, et al. Intravascular origin of metastasis from the proliferation of endothelium-attached tumor cells: a new model for metastasis. *Nat Med*. 2000; 6:100–102. [PubMed: 10613833]
17. Ma C, Wang X-F. In Vitro Assays for the Extracellular Matrix Protein-Regulated Extravasation Process. *Cold Spring Harbor Protocols*. 2008; 2008 pdb.prot5034-, doi:10.1101/pdb.prot5034.
18. Swirski FK, et al. Identification of splenic reservoir monocytes and their deployment to inflammatory sites. *Science (New York, N.Y.)*. 2009; 325:612–616. doi:325/5940/612 [pii]10.1126/science.1175202.
19. Gerber HP, et al. VEGF is required for growth and survival in neonatal mice. *Development*. 1999; 126:1149–1159. [PubMed: 10021335]
20. Huang Y, et al. Pulmonary vascular destabilization in the premetastatic phase facilitates lung metastasis. *Cancer research*. 2009; 69:7529–7537. doi:0008-5472.CAN-08-4382 [pii]10.1158/0008-5472.CAN-08-4382. [PubMed: 19773447]

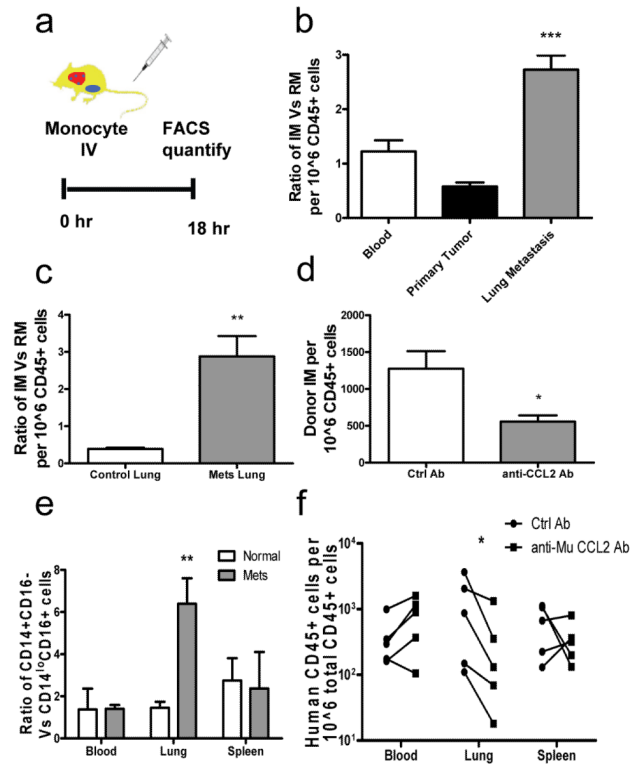
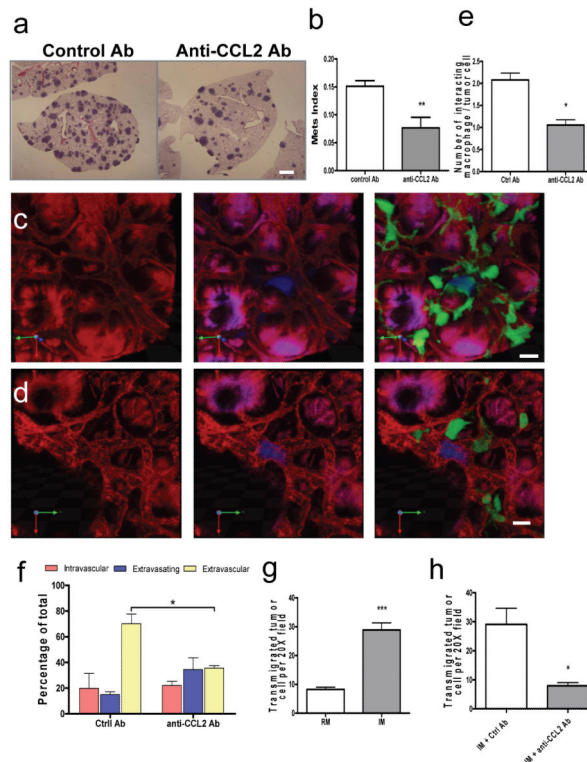


Figure 1.

Pulmonary metastases preferentially recruit inflammatory monocytes through CCL2.

a, Schematic for monocyte adoptive transfer into PyMT tumor mice with pulmonary metastases. **b**, Ratio of IM versus RM in different tissues of recipient mice bearing PyMT tumors and metastases. $n=6$, $p<0.0001$. **c**, Ratio of IM versus RM in control lung and lungs with i.v. injected Met-1 cells 7 hours before. $n=4$, $p=0.0039$. **d**, Relative donor IMs recruited in lungs challenged with Met-1 cells for 7 hours with control or anti-mouse CCL2 antibody treatment. $n=3$, $p=0.045$. **e**, Ratio of adoptively transferred CD14⁺CD16⁻ and CD14^{lo}CD16⁺ human monocytes recruited into normal mice (open bars) and mice challenged with LM2 cells (solid bars) for 7 hours, $n=5$, $p=0.0163$. **b-e**, All bar = mean + s.e.m **f**, Number of adoptively transferred human CD14⁺CD16⁻ monocytes that migrated into different tissues of mice challenged with LM2 cells via i.v. injection with control or anti-mouse CCL2 Ab treatment $n=5$, $p=0.016$, each line connects data from same donor.

**Figure 2.**

CCL2-recruited monocytes promote metastatic seeding.

a, Representative H&E stained sections showing Met-1 metastasis with Ab treatment. Bar=1 mm. **b**, Met-1 metastasis (Mets) burden with different Ab treatment. $n=6$, $p=0.006$. **c** and **d**, Representative snapshots of 3D reconstructed confocal images of tumor cells (blue) and macrophages (green) in lung vasculature (red) 24 hours after tumor cell tail vein injection in mice treated with control (**c**) or anti-mouse CCL2 Ab (**d**). Bar = 20 μ m. **e**, Number of macrophage-tumor cell interactions in mice with Ab treatment. **f**, Tumor cell extravasation in mice with different Ab treatment. (**e**, $p=0.0066$ and **f**, $p=0.00163$ are based upon 3D images of 15-20 tumor clusters per mouse, $n=3$ mice/group.) **g**, Number of transmigrated Met-1 cells in presence of RMs or IMs. $n=5$, $p<0.0001$. **h**, Number of transmigrated Met-1 cells in presence of IMs with different Ab. $n=3$, $p=0.0204$. All bars shown are mean + s.e.m.

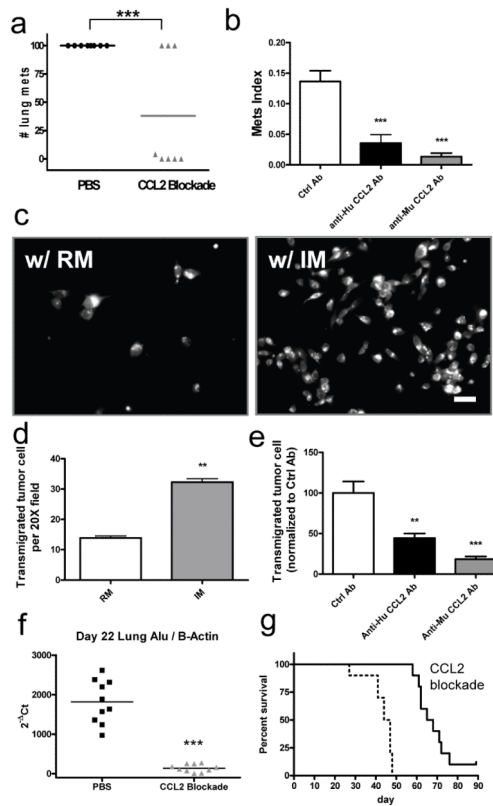
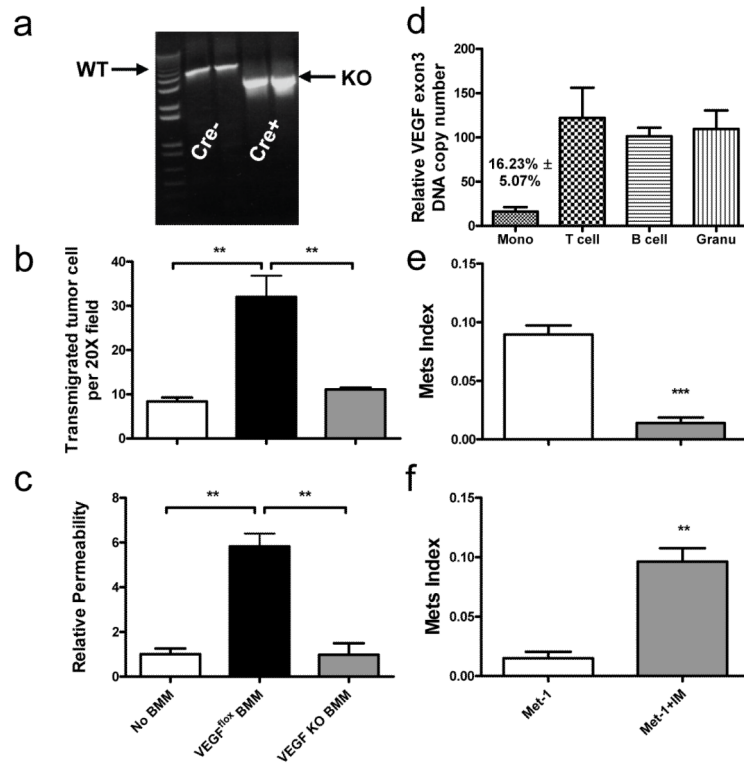


Figure 3.

Tumor cell and host CCL2 promote metastatic seeding.

a, Number of spontaneous pulmonary metastases from orthotopic MDA-MB-231 tumors with total CCL2 blockade or control treatment. Bar equals mean, $n = 8/\text{group}$, $p < 0.001$. **b**, Mets burden of i.v. injected 4173 cells with different Ab treatment. $n = 6$, $p = 2.14 \times 10^{-5}$. Bar equals mean + s.e.m. **c**, Representative fluorescent micrograph of transmigrated human 4173 cells pre-stained with cell tracker dye in the presence of different monocyte populations. Bar equals 20 μm . **d**, Number of transmigrated 4173 cells in presence of IMs or RMs. Bar equals mean + s.e.m. of 3 experiments with duplicates. **e**, Relative number of transmigrated 4173 cells in presence of IMs with control, anti-human or anti-mouse CCL2 Ab normalized to average of control Ab which is arbitrarily set to 100. Bar represents mean + s.e.m. of 5 experiments with duplicates. One way anova with Bonferroni's multiple comparison test, $**p < 0.01$, $***p < 0.001$. **f and g**, CCL2 blockade starting from 2 days after MDA-MB-231 cells i.v. injection significantly reduces Mets burden as measured by realtime PCR of human Alu repeats normalized to mouse β actin on day 22 (**f**, $n = 10$, $***p < 0.001$) and prolongs survival (**g**, $n = 10$, $p < 0.001$).

**Figure 4.**

Monocyte-specific ablation of VEGF blocks pulmonary seeding.

a, PCR of VEGF exon3 of BMMs of *VEGF^{fl/fl}* mice with or without *Csf1r-Mer-iCre-Mer* transgene treated with 4-hydroxytamoxifen. Wild type (WT) and knockout (KO) bands are indicated. **b and c**, Number of trans-endothelial migrated Met-1 cells without BMM (**b**) and albumin permeability of endothelial monolayer (**c**), with WT or VEGF knockout BMMs. n=3 with duplicates. **p<0.01 with ANOVA. **d**, Relative VEGF exon 3 copy number in leukocytes from the peripheral blood of tamoxifen treated *VEGF^{fl/fl};Csf1r-Mer-iCre-Mer* and *VEGF^{fl/fl}* mice. **e**, Met-1 Mets burden in *VEGF^{fl/fl}* mice with or without *Cre* with same tamoxifen treatment. n=6, p=0.0004. **f**, Met-1 Mets burden in *VEGF^{fl/fl};Csf1r-Mer-iCre-Mer* mice with tamoxifen treatment with or without IM co-injection. n=6, p<0.0001. All data are mean+s.e.m.